



Host-Guest Binding Hierarchy within Redox- and Luminescence-Responsive Supramolecular Self-Assembly Based on Chalcogenide Clusters and γ -Cyclodextrin

Anton A Ivanov, Clement Falaise, Pavel A Abramov, Michael A Shestopalov, Kaplan Kirakci, Kamil Lang, Mhamad A Moussawi, Maxim N Sokolov, Nikolay G Naumov, Sébastien Floquet, et al.

► To cite this version:

Anton A Ivanov, Clement Falaise, Pavel A Abramov, Michael A Shestopalov, Kaplan Kirakci, et al.. Host-Guest Binding Hierarchy within Redox- and Luminescence-Responsive Supramolecular Self-Assembly Based on Chalcogenide Clusters and γ -Cyclodextrin. *Chemistry - A European Journal*, 2018, 24 (51), pp.13467-13478. 10.1002/chem.201802102 . hal-01863768

HAL Id: hal-01863768

<https://univ-rennes.hal.science/hal-01863768>

Submitted on 29 Aug 2018

HAL is a multi-disciplinary open access archive for the deposit and dissemination of scientific research documents, whether they are published or not. The documents may come from teaching and research institutions in France or abroad, or from public or private research centers.

L'archive ouverte pluridisciplinaire **HAL**, est destinée au dépôt et à la diffusion de documents scientifiques de niveau recherche, publiés ou non, émanant des établissements d'enseignement et de recherche français ou étrangers, des laboratoires publics ou privés.

FULL PAPER

Host-Guest Binding Hierarchy within Redox- and Luminescence Responsive Supramolecular Self-Assembly Based on Chalcogenide Clusters and γ -Cyclodextrin

Anton A. Ivanov,^[a, b, c] Clément Falaise,^[c] Pavel A. Abramov,^{*[a, d]} Michael A. Shestopalov,^[a, b, d] Kaplan Kirakci,^[e] Kamil Lang,^[e] Mhamad A. Moussawi,^[c] Maxim N. Sokolov,^[a, d] Nikolay G. Naumov,^[a, d] Sébastien Floquet,^[c] David Landy,^[f] Mohamed Haouas,^{*[c]} Konstantin A. Brylev,^[a, d] Yuri V. Mironov,^[a, d] Yann Molard,^[g] Stéphane Cordier^[g] and Emmanuel Cadot^{*[c]}

Abstract: Water-soluble salts of anionic $[Re_6Q_8(CN)_6]^{4-}$ ($Q = S, Se, Te$) chalcogenide octahedral rhenium clusters react with γ -cyclodextrin (γ -CD) producing a new type of inclusion compounds. Crystal structures determined through single-crystal X-ray diffraction analysis revealed supramolecular host-guest assemblies resulting from close encapsulations of the octahedral cluster within two γ -CDs. Interestingly, nature of the inner Q ligands influences strongly the host-guest conformation. The cluster $[Re_6S_8(CN)_6]^{4-}$ interacts preferentially with the primary faces of the γ -CD while the bulkier clusters $[Re_6Se_8(CN)_6]^{4-}$ and $[Re_6Te_8(CN)_6]^{4-}$ exhibit specific interactions with the secondary faces of the cyclic host. Furthermore, analysis of the crystal packing reveals additional supramolecular interactions that lead to 2D infinite arrangements with $[Re_6S_8(CN)_6]^{4-}$ or to 1D “bamboo-like” columns with $[Re_6Se_8(CN)_6]^{4-}$ and $[Re_6Te_8(CN)_6]^{4-}$ species. Solution studies, using multinuclear NMR methods, ESI-MS and Isothermal titration calorimetry (ITC) corroborates nicely the solid state investigations showing that supramolecular pre-organization is retained in aqueous solution

even in diluted conditions. Furthermore, ITC analysis showed that host-guest stability increases significantly ongoing from S to Te. At last, we report herein that deep inclusion alters significantly the intrinsic physical-chemical properties of the octahedral clusters, allowing redox tuning and near IR luminescence enhancement.

Introduction

Self-assembly processes and structures driven by weak non-covalent interactions give rise to innumerable chemical events in living organisms.^[1] Resulting supramolecular organizations are of prime importance in functioning compartmentalized systems such as enzymes which conjugate sophisticated structures with highly specific molecular recognition involved within cascade catalytic mechanisms.^[2] Thereby, self-assembly in biological systems have been often used as guiding models for designing “bio-inspired” sophisticated supramolecular complexes. Such a biomimicking approach has led to many efficient innovative systems in the field of artificial photosynthesis,^[3] catalysis^[4] or drug delivery.^[5]

Actually, development of new composite materials by controlling nature, specificity and strength of intermolecular interactions corresponds to an efficient strategy for the design of hierarchical hybrid assemblies with novel structures and emergent properties.^[6] In this context, host-guest type supramolecular arrangements are of particular interest, especially those that use cyclodextrins (CDs) as functional cavitand. Cyclodextrins are symmetrical macrocyclic cavitands consisting of six, seven, or eight glucopyranoside units named α -, β -, or γ -CD, respectively.^[7] Due to their crown-like hydrophilic portals and hydrophobic inner cavity, CDs have received much interest as host receptors in encapsulation processes and hybrid assemblies.^[5b, 8] Their remarkable structural features have led to wide applications in separation, analysis, selective catalysis, materials and life sciences.^[9] Moreover, impressive inclusion capabilities and resulting synthetic host-guest systems create favorable conditions for substrate activation in the hydrophobic cavities of CDs via non-covalent interactions, thus mimicking enzymatic chemical reactions.^[9b] Usually such bioinspired systems involve coordination^[10] or organometallic^[11] complexes closely embedded within the hydrophobic pocket of CDs. Nevertheless, little is known about supramolecular interactions of CDs with polynuclear species, such as metal clusters. Recently inclusion complexes with polyoxometalates^[12] and octahedral clusters^[12b, 13] were reported. Their structural investigations clearly demonstrate that stoichiometry,

- [a] A. A. Ivanov, Dr. P. A. Abramov, Dr. M. A. Shestopalov, Prof. Dr. M. N. Sokolov, Dr. N. G. Naumov, Dr. K. A. Brylev, Dr. Y. V. Mironov
Nikolaev Institute of Inorganic Chemistry SB RAS
3 acad. Lavrentiev ave., 630090 Novosibirsk (Russia)
E-mail: abramov@niic.nsc.ru
- [b] A. A. Ivanov, Dr. M.A. Shestopalov
The Federal Research Center of Fundamental and Translational Medicine
2 Timakova st., 630117 Novosibirsk (Russia)
- [c] A. A. Ivanov, Dr. C. Falaise, Dr. M. A. Moussawi, Dr. S. Floquet, Dr. M. Haouas, Prof. Dr. E. Cadot
Institut Lavoisier de Versailles, CNRS, UVSQ, Université Paris-Saclay
45 avenue des Etats-Unis, 78035 Versailles (France)
E-mail: emmanuel.cadot@uvsq.fr, mohamed.haouas@uvsq.fr
- [d] Dr. P. A. Abramov, Dr. M. A. Shestopalov, Prof. Dr. M. N. Sokolov, Dr. N. G. Naumov, Dr. K. A. Brylev, Dr. Y. V. Mironov
Novosibirsk State University
2 Pirogova st., 630090 Novosibirsk (Russia)
- [e] Dr. K. Kirakci, Prof. K. Lang
Institute of Inorganic Chemistry of the Czech Academy of Sciences
Husinec-Řež 1001, 250 68 Řež (Czech Republic)
- [f] Prof. D. Landy
Unité de Chimie Environnementale et Interactions sur le Vivant (UCEIV, EA 4492)
145, Avenue Maurice Schumann, MREI 1, 59140 Dunkerque (France)
- [g] Dr. Y. Molard, Dr. S. Cordier
Institut des Sciences Chimiques de Rennes, UMR 6226 CNRS, Université de Rennes 1
Avenue du Général Leclerc, 35042 Rennes (France)

Supporting information for this article is given via a link at the end of the document.

Accepted Manuscript

FULL PAPER

conformation and spatial arrangement of the resulting host-guest adducts are highly sensitive to the nature of the guest, leading to highly contrasted behavior in solution, ranging from extremely labile assembly with $[Re_6S_8(H_2O)_6]^{2+}$ up to dynamically frozen supramolecular arrangement with $[Ta_6Br_{12}(H_2O)_6]^{2+}$ species.^[12b, 13a] For instance, encapsulation of the $[Ta_6Br_{12}(H_2O)_6]^{2+}$ cluster within two γ -CD molecules provokes spectacular changes in the redox potential, thereby showing that physical-chemical properties of the cluster are highly sensitive to its proximal environment even in the absence of specific coordinative interactions. In this context, supramolecular host-guest systems involving cluster-based assemblies and CDs are of prime interest in biology or medicine. Actually, electron-rich octahedral clusters exhibit highly appealing optical properties such as phosphorescence in the NIR region triggered by UV, visible light or even X-ray irradiation^[14] with lifetimes up to several hundred microseconds and exceptionally high quantum yield, making this class of material highly relevant for bioimaging^[15] or biolabelling applications.^[16] Additionally, this class of compounds exhibit high radiodensity due to close packing of heavy elements in the cluster core $\{M_6Q_8\}$ with M = Mo, W or Re; Q = Se, Te, Br or I which is a pre-requisite for X-ray contrast agents and thereby useful for bimodal bioimaging.^[17] Moreover, octahedral clusters behave also as potential antitumoral and antimicrobial agents due to their ability to generate singlet oxygen upon photoirradiation.^[18] Thus, cumulative properties such as luminescence, redox activity, amenability to unique chemical transformations make this class of multifunctional compounds highly relevant for the design of efficient bioactive systems. As cyclodextrins are well-known to improve biocompatibility and bioavailability of drug molecules,^[19] their combination with $\{M_6Q_8\}$ octahedral based-clusters paves the way toward a novel class of agents highly relevant for bioimaging, diagnostic or therapy.

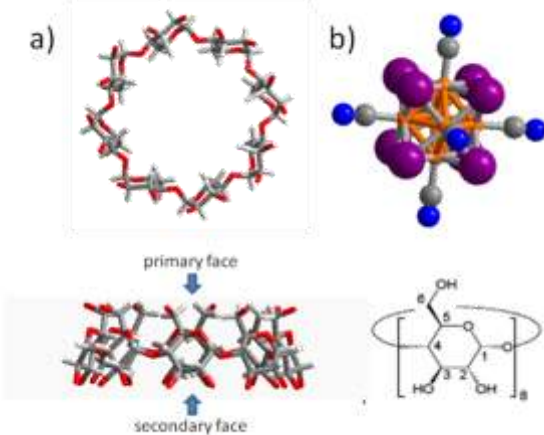


Figure 1. Structural representation of the molecular components used as building blocks: a) γ -cyclodextrin $C_{48}H_{80}O_{40}$ (γ -CD) resulting from the condensation of eight glycopyranose units $\{C_6H_{10}O_5\}$. The macrocycle delimits the primary face (lined by the eight methanolic groups) and by the opposite secondary face (lined by sixteen hydroxyl groups). b) octahedral cluster $[Re_6Q_8(CN)_6]^{4-}$ built from six rhenium Re^{III} ions located at the octahedron corners and mutually linked through metal-metal bonds ($Re-Re = 2.64-2.69\text{\AA}$). The resulting $\{Re_6\}$ core is face capped by eight μ_3 -Q ligands (with $Q = S$, Se and Te) while the coordination sphere of the six Re centers is completed by a cyano ligand in apical position. Color code: orange = rhenium, violet = Q (S, Se or Te), grey = carbon, blue = nitrogen, red = oxygen, white = hydrogen.

In this paper we report on the formation of host-guest supramolecular complexes in aqueous solution involving γ -CD as host and anionic $[Re_6Q_8(CN)_6]^{4-}$ ($Q = S$, Se , Te) clusters as guests (Figure 1). Structural models of supramolecular adducts have been obtained through single-crystal X-ray diffraction analysis, revealing the deep inclusion of the $[Re_6Q_8(CN)_6]^{4-}$ clusters within two γ -CD capsules. Furthermore, solution studies, using ESI-MS and multinuclear NMR techniques confirmed that supramolecular interactions are maintained in aqueous solution. Nevertheless, isothermal titration calorimetry experiments (ITC) revealed that efficiency of the supramolecular recognition process is strongly dependent upon the nature of the μ_3 -chalcogenide ion ($Q = S$, Se or Te) in the $\{Re_6Q_8\}^{2+}$ cluster core. Such a contrasting behavior is also nicely supported by NMR conclusions that balance from highly labile associations with $Q = S$, Se to robust frozen arrangements with $Q = Te$. Besides, we report herein that supramolecular γ -CD shells have noteworthy influences upon the electrochemical and luminescence properties of the embedded clusters, thus providing new arguments and opportunities for their deliberate integration within functioning systems useful in the area of biotechnological applications.

Results and Discussion

Formation of the γ -CD based adducts

Isolation of the supramolecular adducts has been carried out through systematic studies using different ratios of alkali salts of octahedral clusters $M_4[Re_6Q_8(CN)_6] \cdot nH_2O$ (with $M = Na$ or K and $Q = S$, Se or Te) and varying procedures of crystallization such as slow evaporation of aqueous solution or vapor diffusion method. In short, this study showed that Se - and Te -containing clusters exhibit high propensity to form the 1:2 supramolecular adduct $\{Re_6Q_8\} \subset (\gamma\text{-CD})_2$, consistent with X-Ray diffraction analysis or NMR solution studies. Compounds **1** and **2**, corresponding to $Na_4[\{Re_6Te_8(CN)_6\} \subset (\gamma\text{-CD})_2] \cdot (\gamma\text{-CD}) \cdot 30H_2O$ and $K_4[\{Re_6Se_8(CN)_6\} \subset (\gamma\text{-CD})_2] \cdot (\gamma\text{-CD}) \cdot 40H_2O$, respectively, were obtained as single-crystals through slow evaporation of aqueous solutions. Conversely, applying similar procedures to the sulfur-containing cluster unit led systematically to formation of colorless cluster-free crystals corresponding to γ -CD, meaning that supramolecular interactions should give labile and highly soluble adducts reluctant to crystallize. Nevertheless, changing the crystallization conditions for slow ethanol vapor diffusion into aqueous solution containing cesium chloride produced single-crystals suitable for XRD. Structural analysis of compound $Cs_4K_8[\{Re_6S_8(CN)_6\} \subset (\gamma\text{-CD})_2] \cdot 2[\{Re_6S_8(CN)_6\}] \cdot 2(\gamma\text{-CD}) \cdot 49H_2O$ (**3**) revealed unexpected host-guest interactions as discussed below.

Single-crystal X-ray analysis

Main crystallographic parameters for structures of compounds **1**, **2** and **3** which involves γ -cyclodextrin and $[Re_6Q_8(CN)_6]^{4-}$ with $Q = Te$, Se or S , respectively, are given in supporting information (SI §2.1, Table S1). X-ray diffraction study revealed three host-guest supramolecular adducts involving γ -CD and octahedral clusters $[Re_6Q_8(CN)_6]^{4-}$ with $Q = Te$, Se or S . Nevertheless, depending upon conditions of crystallization and the nature of the octahedral-type cluster, CD:cluster stoichiometry and supramolecular interactions observed in the crystal structures differ strikingly.

FULL PAPER

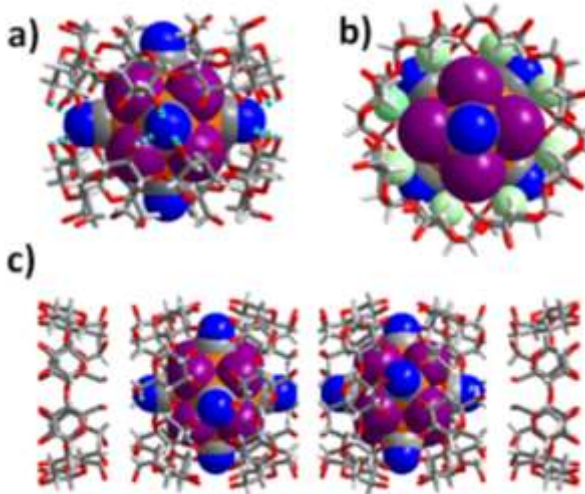


Figure 2. Mixed representations of the solid state structure of the supramolecular host-guest $\{[\text{Re}_6\text{Q}_8(\text{CN})_6]\subset(\gamma\text{-CD})_2\}^4$ complex with $\text{Q} = \text{Se}$ or Te : a) side view showing the hydrogen bonding between the equatorial cyano groups and the hydroxyls of the primary faces of the CDs; b) top view highlighting close interactions between inner H-3 hydrogen (pale-green sphere) and four Q ligands (violet sphere) with $\text{H}\cdots\text{Q} = 3.1\text{--}3.5 \text{ \AA}$; c) focus on the linear “bamboo-like” arrangement running along c axis.

Structural analysis of $\text{Na}_4\{[\text{Re}_6\text{Te}_8(\text{CN})_6]\subset(\gamma\text{-CD})_2\}\cdot(\gamma\text{-CD})\cdot30\text{H}_2\text{O}$ and $\text{K}_4\{[\text{Re}_6\text{Se}_8(\text{CN})_6]\subset(\gamma\text{-CD})_2\}\cdot(\gamma\text{-CD})\cdot40\text{H}_2\text{O}$ (noted **1** and **2**, respectively) revealed two isostructural compounds which contain the octahedral cluster $[\text{Re}_6\text{Q}_8(\text{CN})_6]^{4-}$ closely embedded into two γ -CDs facing their wider rim (secondary face) and $\{\text{Re}_6\text{Q}_8\}^{2+}$ clusters range within those usually observed (see SI §2.2, Table S2). In addition, some weak intermolecular interacting mutually through hydrogen bonds ($\text{O}\cdots\text{O} \sim 2.8\text{--}3.1 \text{ \AA}$) (see Figure 2a). Geometrical parameters of the encapsulated $\{\text{Re}_6\text{Q}_8\}^{2+}$ clusters range within those usually observed (see SI §2.2, Table S2). In addition, some weak intermolecular interactions can be identified within the solid state structures contributing to the stability of the supramolecular host-guest arrangements. Each equatorial cyano group interacts through hydrogen bonds with the three closest hydroxyl groups of the wider rim of CD giving $\text{N}\cdots\text{O}$ distances in the $2.8\text{--}3.0 \text{ \AA}$ range while Q inner ligands ($\text{Q} = \text{Se}$ or Te) participate also to the supramolecular cohesion (see Figures 2a-b), giving close contacts with inward-directed hydrogen H-3 labelled in the γ -CD ($\text{H}\cdots\text{Se} = 3.2\text{--}3.5 \text{ \AA}$ and $\text{H}\cdots\text{Te} = 3.1\text{--}3.4 \text{ \AA}$). Furthermore, in the crystal packing, two supramolecular adducts $\{[\text{Re}_6\text{Q}_8(\text{CN})_6]\subset(\gamma\text{-CD})_2\}^{4-}$ stack together through their primary faces along the [001] direction to give the typical tubular arrangement. At last, both sides are symmetrically closed by two additional free γ -CDs (see Figure 2c). The cohesion within such large enchainment is mainly ensured by a network of direct hydrogen bonding that interconnects alternately secondary rims and primary rims ($\text{O}\cdots\text{O} = 2.7\text{--}3.0 \text{ \AA}$). This arrangement appears very similar to that reported previously by Nau et al. on inclusion complexes involving γ -CD and $[\text{B}_{12}\text{Br}_{12}]^{2-}$ dodecaborate cluster.^[20] Such similarities mean that in this case, crystal packing is mainly imposed by structural properties of the bulky γ -CD, while water molecules and disordered counter-cations (Na^+ or K^+ for $\text{Q} = \text{Se}$

or Te , respectively) should be probably distributed within large voids between the tubular assemblies.

X-ray diffraction structural analysis of compound **3** containing the $[\text{Re}_6\text{S}_8(\text{CN})_6]^{4-}$ octahedral type-cluster and γ -CD is graphically shown in Figure 3. Crystal structure of **3** reveals also host-guest arrangements built on the cluster unit bicapped by two γ -CD molecules, but here, both γ -CD face their two primary faces (see Figure 3a), instead of the secondary faces as observed in structure **1** and **2**. It should be worth remarking that such host-guest disposition was already reported in systems involving bulky guests such as Keggin $[\text{PMo}_{12}\text{O}_{40}]^{3-}$ or Dawson $[\text{P}_2\text{W}_{18}\text{O}_{62}]^{6-}$ anions.^[12a, 12c] Furthermore, the relative disposition of the cluster within the two opposite CDs depicted in **3** differs from that observed in **1** or **2**. The equatorial plane of the $[\text{Re}_6\text{S}_8(\text{CN})_6]^{4-}$ cluster lined by four *in plane* cyano groups is perpendicularly directed with respect to the faces of the γ -CDs while the two remaining opposite axial cyano ligands point between the two primary rings of the γ -CDs. Nonetheless, complete structural description of crystal **3** should mention an additional type of interactions wherein the cluster unit and γ -CD stack together to form regular planes (see Figure 3b). In such arrangement the cavity of γ -CD remains free while the clusters interact with the outer part of γ -CD torus (see Figure 3b). In summary, compound **3** exhibits an overall stoichiometry cluster: γ -CD = 3:4 and contains two types of supramolecular interactions, leading to a quite typical 1:2 discrete host-guest arrangement involving the primary faces of the γ -CD tori. The second type of interaction appears less specific and allows the formation of regular plane paved from the strict alternation of $[\text{Re}_6\text{S}_8(\text{CN})_6]^{4-}$ anion and γ -CD tori. At last, the counter cations, K^+ and Cs^+ , have been found and appear mainly located in the vicinity of the hydroxyl groups of the γ -CD and, thereby, quite far from the anionic clusters (not shown).

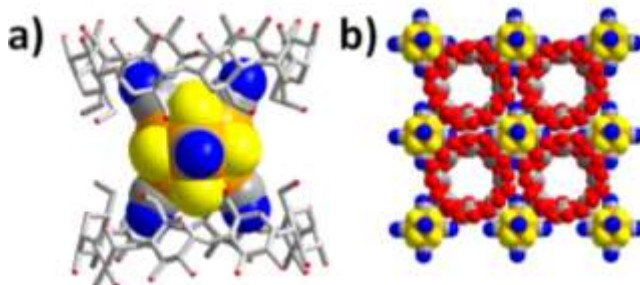


Figure 3. Mixed representations of the solid state structure of compound **3** containing the $[\text{Re}_6\text{S}_8(\text{CN})_6]^{4-}$ anion and γ -CD involved within two types of interactions: a) conventional discrete supramolecular host-guest arrangement showing two primary faces embedding the inorganic cluster; b) view highlighting close packing of clusters and γ -CDs within a 2D infinite arrangement.

Solution studies

The solution behavior was investigated by a set of complementary techniques such as multinuclear ^1H , ^{13}C , ^{77}Se and ^{125}Te NMR spectroscopy, UV-Vis spectroscopy, ITC, and ESI-mass spectrometry. ITC experiments were conducted to determine the thermodynamic parameters of the encapsulation process.

FULL PAPER

NMR study

Multinuclear NMR provides complementary informative analytical tools able to track supramolecular effects using available NMR probes either from the host (^1H or ^{13}C) or from the guests with ^{77}Se and ^{125}Te .^[21] ^1H NMR titrations were conducted for all clusters Q = S, Se or Te allowing to determine averaged cluster:CD stoichiometry in solution (Job plot analysis) and in some extend to give some insights about structures of supramolecular aggregates formed in aqueous solutions. ^1H NMR titrations are shown in Figures 4a-c, and experimental details given in supporting information section. In the case of Te-containing cluster (Figure 4a), appearance of several new signals feature complex formation in a nearly frozen situation on the NMR time scale. For instance, H1 and H5 resonances clearly reflect the formation of the 1:2 host-guest arrangement in aqueous solution (see Figure 4a). Nevertheless, combination of slow exchange dynamics and restricted molecular movement due to aggregation cause significant line broadening (see, SI §3.1, Figure S2). In case of S or Se clusters, ^1H NMR patterns behave differently, without excessive line broadening upon introducing up to 12 cluster equivalents (see Figures 4b and 4c), concomitant with the gradual variations of the ^1H NMR resonances. These results are consistent with highly labile associations (extreme narrowing situation on the NMR time scale). These observations confirm quite strong interaction of the three clusters (Q = Te, Se or S) with the γ -CD torus which should correspond to inclusion complexes.

For Te- and Se-containing clusters, most important shifts for the inner H3 protons supported by NMR titration and Job plot analysis appear fairly consistent with the solid state structure **3** showing the $\{[\text{Re}_6\text{Q}_8(\text{CN})_6] \subset (\gamma\text{-CD})_2\}^{4-}$ arrangement (see Figure 2a). In addition, the existence of the 1:2 supramolecular arrangements in diluted solutions has been confirmed by ITC experiments. For the S-containing cluster, NMR analysis shows clearly that in addition to H3 chemical shift variations, H5 inner proton appears also mostly affected by the inclusion process. Besides, NMR analysis is also consistent with 1:1 average stoichiometry nicely confirmed by ITC (see SI § 3.2, Figures S3 and S4a). As these results differ from those obtained from X-ray diffraction analysis (see Figure 3), they could arise from weak selectivity of the supramolecular recognition process due to the smaller sized sulfur-containing cluster. Size volume calculation within the $[\text{Re}_6\text{Q}_8(\text{CN})_6]^{4-}$ series gives 387, 419 and 473 \AA^3 for Q = S, Se and Te, respectively. Weak selectivity and affinity (see ITC results below) lead to predominant 1:1 associations in solution that could occur either from the secondary face (affecting the H3 inner proton) or from the primary face of the torus (leading to the H5 shift resonance).

Evidence for the inclusion complex formation is also provided by ^1H DOSY NMR. The self-diffusion coefficient D of γ -CD drops from ca. 250 $\mu\text{m}^2/\text{s}$ for the free γ -CD^[21b] to ca. 220, 210, and 190 $\mu\text{m}^2/\text{s}$ for CD-[$\text{Re}_6\text{Q}_8(\text{CN})_6$]⁴⁻ solutions for Q = S, Se, and Te respectively, upon increasing the cluster to CD ratio (for further details, see SI, §3.3, Figure S5). However D changes are moderate because the hydrodynamic radii of supramolecular adducts are dominated mainly by the CD host, but significant decreases of self-diffusion coefficients indicate formation of labile host-guest aggregates.

^{77}Se and ^{125}Te NMR studies of solutions containing $[\text{Re}_6\text{Q}_8(\text{CN})_6]^{4-}$ (Q = Se, Te) and γ -CD have been conducted at

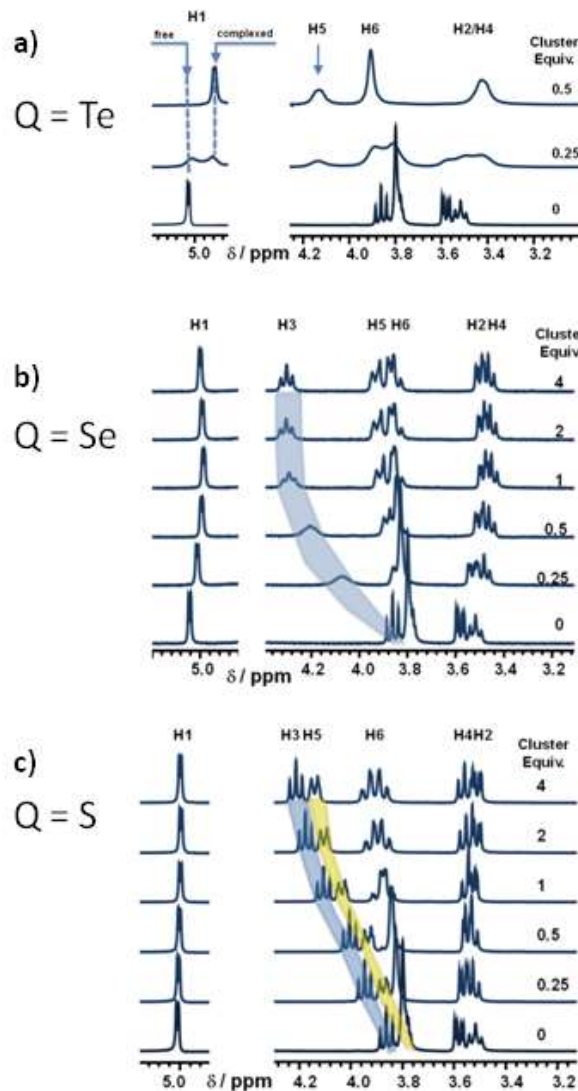


Figure 4. ^1H NMR spectra resulting of the titration of 3 mmol. L^{-1} aqueous solution of γ -CD by $[\text{Re}_6\text{Q}_8(\text{CN})_6]^{4-}$ cluster. a) Q = Te; b) Q = Se and c) Q = S.

fixed cluster concentration (shown in Figure 5). In the case of Se cluster, a single signal is observed shifting progressively from $\delta = -389$ ppm to the limiting value at -392.6 ppm (see Figure 5b). This indicates a fast exchange regime between the different cluster species, i.e. solvated or embedded within γ -CD. Besides, Job plot using the ^{77}Se NMR data (see SI, §3.2, Figure S3) confirms the formation of the predominant 1:2 type complex in aqueous solution, still consistent with the solid state structure and ^1H NMR analysis. Conversely, complexation of the $[\text{Re}_6\text{Te}_8(\text{CN})_6]^{4-}$ cluster leads to two ^{125}Te NMR resonances at $\delta = -1127$ ppm and $\delta = -1165$ ppm according to the slow chemical exchange regime observed by ^1H NMR. While ^{125}Te NMR titration gives also direct evidence for the 1:2 stoichiometry of the frozen CD-cluster conformation (see SI, §3.1 and 3.2, Figure S4b), such an experiment allows evidencing the formation of the highly labile 1:1 complex which causes the significant broadening of the $\delta = -1127$ ppm ^{125}Te resonances observed for CD/cluster ratio in the 0-1 range (see Figure 5a).

FULL PAPER

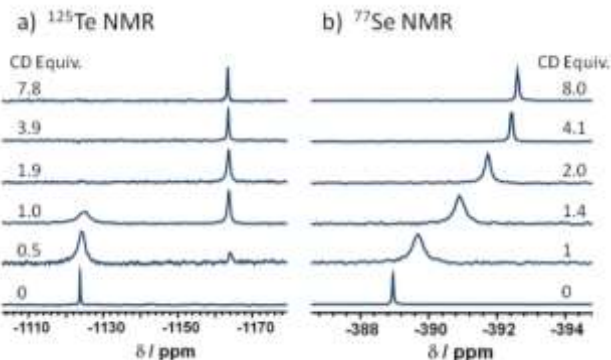


Figure 5. (a) ^{125}Te NMR spectra of 6 mM solution of $[\text{Re}_6\text{Te}_8(\text{CN})_6]^{4-}$ and (b) ^{77}Se NMR spectra of 24 mM solution of $[\text{Re}_6\text{Se}_8(\text{CN})_6]^{4-}$, containing various amounts of γ -CD.

At last, ^{13}C NMR spectra were also recorded to monitor the inclusion complex formation (see SI, §3.4, Figure S6) through the conformational changes of the γ -CD macrocycle. The spectra of Te cluster system showed broad signals due to slow exchange regime that makes the measurement and interpretation of the spectra difficult. However, narrow signals are obtained for S and Se cluster systems and their measurements are much easier. Actually, variations of ^{13}C NMR chemical shifts reflect mainly the macrocycle distortions when accommodating the guest rather than the through-space host-guest contacts, as observed with ^1H .^[21b] Featuring the mode of encapsulation, the carbon C1 and C4 atoms of the ring exhibit an opposite chemical shift variation (see SI, §3.4). These C1 and C4 atoms behave as hinge within the CD backbone, allowing in some extent expansion / contraction of the opposite rims. According to the solid state structure, host-guest interactions should provoke expansion of the secondary rim and the concomitant contraction of the primary one when $\text{Q} = \text{Se}$ while opposite trend holds for $\text{Q} = \text{S}$. It should be worth remarking that chemical shifts of the remaining C2, C3, C5 and C6 carbon atoms exhibits similar variation whatever the nature of the chalcogenide inner ligands ($\text{Q} = \text{S}$ or Se). Furthermore, the ^{13}C NMR chemical shift of the outer cyano ligands appears quite unaffected for the sulfur-containing cluster while it undergoes significant deshielding when $\text{Q} = \text{Se}$. Such a difference arises probably from the hydrogen bonding network similar to that detected in the solid state which involves the equatorial cyano groups and the sixteen hydroxyl groups from the secondary rim (see Figure 2a). Such types of supramolecular interaction are prominent with the $[\text{Re}_6\text{Se}_8(\text{CN})_6]^{4-}$ and fully cancelled in the host-guest conformations involving the S-containing cluster $[\text{Re}_6\text{S}_8(\text{CN})_6]^{4-}$ and the primary faces of the CDs (see Figure 3a).

ESI-MS studies

Solutions containing cluster and γ -CD have been investigated using ESI-MS. The results corroborate entirely the hypotheses and interpretations formulated from solid state analysis and multinuclear NMR investigations. In each case, the ESI-MS spectrum contains the 1:1 and 1:2 supramolecular complexes (see SI, §4, Figure S7 for further details). For $\text{Q} = \text{S}$ or Se , the 1:1 and 1:2 adducts are associated to two Na^+ cations to give $(\text{Na}_2[\text{Re}_6\text{Q}_8(\text{CN})_6]\subset(\gamma\text{-CD})_x)^{2-}$ species with $x = 1$ or 2 while for $\text{Q} = \text{Te}$

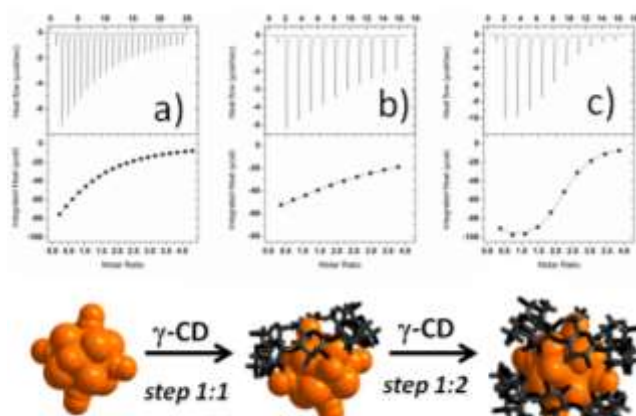


Figure 6. ITC thermograms (upper part) and isotherms (lower part) at 283 K corresponding to titration of solution of $\text{K}_4[\text{Re}_6\text{Q}_8(\text{CN})_6]$ by γ -CD: a) $\text{Q} = \text{S}$; b) $\text{Q} = \text{Se}$ and c) $\text{Q} = \text{Te}$. They have been interpreted as the result of formation of 1:1 and 1:2 supramolecular adducts in two consecutive steps, except for $\text{Q} = \text{S}$ where the 1:2 step was found negligible (see Table 1).

= Te, the 1:1 and 1:2 adducts are associated to one proton in $\{\text{H}[\text{Re}_6\text{Te}_8(\text{CN})_6]\subset(\gamma\text{-CD})_x\}^{3-}$ with $x = 1, 2$.

Isothermal calorimetric titration

ITC experiments were carried out to give thermodynamic insights about interactions between the γ -CD and the $[\text{Re}_6\text{Q}_8(\text{CN})_6]^{4-}$ clusters as function of the nature of the chalcogenide inner ligand S, Se or Te. Selected ITC thermograms and isotherms obtained at 283 K are shown Figure 6 while full detailed data and related analytical treatments are given in supporting information (SI, §5). ITC results including binding constants, enthalpy $\Delta_r H^\circ$ and entropy $\Delta_r S^\circ$ are given at 298 K in Table 1. They were analyzed using a two-site binding model involved within a sequential process, except for S-containing cluster for which the second 1:2 step is found negligible. For all the complexes, supramolecular binding is invariably an enthalpically driven process but as the size of the Q ligand increases from S to Te, the enthalpy of the complexation tends to decrease gradually. Such a tendency is exactly opposite to that observed by Nau et al. with dodecaborate $[\text{B}_{12}\text{X}_{12}]^{2-}$ cluster ($\text{X} = \text{Cl}, \text{Br}$ or I), who reasoned, logically, that such a behavior is in line with increasing dispersion interactions (see Table 1 and Figure 7).^[20] Such an apparent discrepancy means that solvation of the rhenium octahedral clusters is mainly governed by the six exposed cyano groups rather than the eight inner Q ligands. In short, increasing the σ donor capability of the Q ligands toward the Re centers ongoing from S to Te weakens the Re-C σ overlap which induces the increase of the {C-N} bond polarization and then the subsequent strengthening of the electrostatic interaction with water molecules of the solvation shell. Such a qualitative explanation was nicely supported by DFT calculations which clearly showed that bonding stabilization comes mainly from σ donation between the cyano outer ligands and the $\{\text{Re}_6\text{Q}_8\}^{2+}$ core, while corresponding M-L bonding energy increases gradually from $\text{Q} = \text{S}$ to Te .^[22] The enthalpic gain appears correlated to entropic penalty according to enthalpy-entropy compensation ($R^2 = 0.96$) that usually hold with CDs-based encapsulation process.^[23] Actually, thermodynamic profile of the rhenium clusters series resembles that of the perhalogenated

FULL PAPER

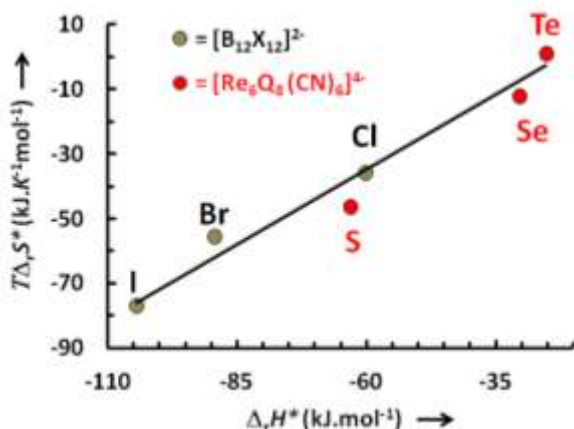


Figure 7. Enthalpy–entropy compensation plot for 1:1 γ -CD complexes with $[Re_6Q_8(CN)_6]^{4-}$ (red circles) compared with those found for $[B_{12}X_{12}]^{2-}$ dodecaborate anions (grey circles) from Ref. [20].

dodecaborates series^[20] and suggests that these ions behave as chaotropic species (water structure breakers). However, as shown in Figure 7, magnitude of the chaotropic character within the $[Re_6Q_8(CN)_6]^{4-}$ series does not increase with the polarizability of the Q ligand, probably due to antagonist influence of the six outer cyano ligands which cancels partially dispersion forces involved within solvation process of the cluster. Nevertheless, the highest affinity was observed with the most bulky anion $[Re_6Te_6(CN)_6]^{4-}$, which optimizes the host-guest dispersion interactions compared to the S- or Se-containing cluster units.

Table 1. Binding constants K involving rhenium octahedral cluster with γ -CD and associated thermodynamic parameters (in kJ·mol⁻¹) at $T = 298$ K.

$[Re_6Q_8(CN)_6]^{4-}$	Step	$K(M^{-1})$	$\Delta_r H^*$	$T\Delta_r S^*$	$\Delta_r G^*$
$Q = S$	1:1	900	-63.2	-46.4	-16.8
	1:2	-	-	-	-
$Q = Se$	1:1	1500	-30.4	-12.3	-18.1
	1:2	300	-56.5	-42.7	-13.8
$Q = Te$	1:1	37700	-25.3	+0.8	-26.1
	1:2	12700	-51.0	-27.7	-23.4

Physical-chemical properties of the host-guest arrangements

Electrochemistry

As $\{Re_6Q_8\}^{2+}$ cores are redox active species, influence of γ -CD upon the electrochemical properties could be examined for the three compounds ($Q = S$, Se or Te). Previous studies reported electrochemical properties of the $[Re_6Q_8(CN)_6]^{4-}$ anions in non-aqueous medium, such as acetonitrile or dichloromethane solvent showing that the 24-electron $\{Re_6Q_8\}^{2+}$ cores undergo a quasi-reversible one-electron transfer leading to the 23-electron oxidized species.^[24] Besides, the oxidizing ability of the $\{Re_6Q_8\}^{2+}$ core was revealed to be dependent on the σ donating character of the Q inner ligands that increases ongoing from S to Te atom.^[25] Surprisingly, electrochemical properties of the

Table 2. Main electrochemical potentials (Volt vs. SCE) for chalcogenide clusters 1-3 and their related inclusion compounds in 25 mmol.L⁻¹ $HClO_4$ aqueous solution at $T = 298$ K.

$[Re_6Q_8(CN)_6]^{4-}$	redox	E_a	E_c	$E_{1/2}$
$Q = S$	Free	0.850	0.785	0.820
	$[Re_6^{\bullet}CD]^{3-} / [Re_6^{\bullet}2CD]^{4-}$	-	-	0.560
$Q = Se$	Free	0.615	0.545	0.580
	$[Re_6^{\bullet}CD]^{3-} / [Re_6^{\bullet}CD]^{4-}$	0.480	-	-
$Q = Te$	Free	0.325	0.255	0.290
	$[Re_6^{\bullet}CD]^{3-} / [Re_6^{\bullet}CD]^{4-}$	0.175	-	-

$\{Re_6Q_8\}^{2+}$ series in aqueous solution have never been reported while many supramolecular processes arise from the remarkable properties of water solvation. Herein, we report for the first time on the electrochemical properties of the $[Re_6Q_8(CN)_6]^{4-}$ anions in aqueous solution and on their deep alteration in the presence of the γ -CD. Electrochemical study of the native $K_4[Re_6Q_8(CN)_6] \cdot nH_2O$ compounds has been carried out in 25 mmol.L⁻¹ $HClO_4$ aqueous solution using various amounts of γ -CD. The corresponding cyclic voltammograms (CVs) are shown in Figures 8a-c and the related data given in Table 2. Each cluster undergoes a mono-electronic wave observed at $E_{1/2} = 0.820$, 0.580 and 0.290 V v.s. SCE for $Q = S$, Se and Te, respectively. Such a trend appears fully consistent with previous results obtained in CH_3CN but a ~ 0.2 V systematic shift toward positive potential was observed in aqueous medium (see Table 2). Furthermore, variation of the anodic (E_a) and cathodic (E_c) peak currents exhibits a fair linear dependence upon square root of the potential scan rate \sqrt{SR} , consistent with a diffusion-controlled electron-transfer kinetic (see SI §6.1, Figure S11). Influence of γ -CD on the electrochemical properties was then investigated showing important changes related to the host-guest structures and solution behavior (see above). Upon gradual addition of γ -CD, the CVs of the sulfur-containing cluster $[Re_6S_8(CN)_6]^{4-}$ retain its reversible shape but undergo a continuous decreasing of its half-wave potential $E_{1/2}$ (see Figure 8a) associated to a substantial reduction of the peak currents. Such observations are consistent with i) fast formation / dissociation of the inclusion complexes that maintains equilibrium conditions over the time scale of the experiment and ii) a more slowly diffusing γ -CD-cluster based species. Furthermore, linear dependence of the anodic and cathodic peak currents upon square root of the potential scan rate \sqrt{SR} is always maintained indicating that γ -CD complexation does not alter the fast kinetic of the electron transfers (see SI §6.1, Figure S12). Surprisingly, no attenuation of these variations was observed up to addition of 50 equivalents of γ -CD indicating that γ -CD is always involved within the redox reactions according to equation 1 and 2 (see SI §6.2, Figure S13). Actually, for large excess of γ -CD up to 10 equivalents, the speciation diagram established from the stability constant $K_{1:1} = 900 M^{-1}$ (see Table 1 and SI §6.3, Figure S14) shows that 1:1 host-guest species is prevalent, thus indicating that equation 2 should govern preferentially the redox process.



FULL PAPER

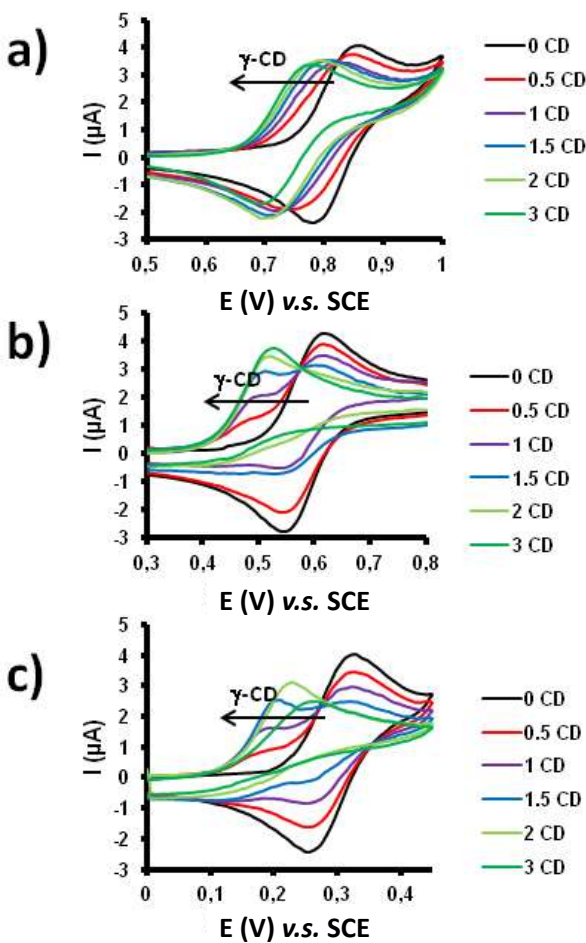


Figure 8. Cyclic voltammetry of the $[\text{Re}_6\text{Q}_8(\text{CN})_6]^{4-}$ anions with $\text{Q} = \text{S}$ (a), Se (b) or Te (c) (0.5 mmol.L^{-1} , 25 mmol.L^{-1} HClO_4 aqueous solution, glassy carbon working electrode, scan rate 50 mV.s^{-1}) in the presence of increasing amounts of $\gamma\text{-CD}$ (from 0 to 3 equivalents).

In such a range of composition, a simple relationship between apparent half-wave potential $E_{1/2}^{\text{app}}$ and $p\text{CD}$ hold as expressed by equation 3 where $p\text{CD} = -\log[\text{CD}]$ and $E_{1/2}^{\text{CD}}$ is the half-wave potential of the redox couple $[(\text{Re}_6)_{\text{ox}} \cdot 2\text{CD}]^{3-} / [(\text{Re}_6)_{\text{red}} \cdot \text{CD}]^{4-}$ associated to equation (2).

$$E_{1/2}^{\text{app}} = E_{1/2}^{\text{CD}} + 0.059 p\text{CD} \quad (3)$$

Actually, equation 3 is experimentally justified by a fair linear function ($R^2 = 0.996$) giving a slope of 0.0585 V per $p\text{CD}$ unit and $E_{1/2}^{\text{CD}} = 0.560 \text{ V}$ (see SI §6.2, Figure S13). At last, equation 4 is then derived easily from the prevalent redox process (2) where $K_{1:1}$ corresponds to the stability constant of the 1:1 host-guest reduced species (see Table 1), β'_2 is the global formation constant related to equation 5 and $E_{1/2}^0$ is the half-wave potential of compound 3 in the absence of $\gamma\text{-CD}$.

$$E_{1/2}^0 = E_{1/2}^{\text{CD}} + 0.059 \log \frac{\beta'_2}{K_{11}} \quad (4)$$

$$[(\text{Re}_6)_{\text{ox}}]^{3-} + 2 \text{ CD} = [(\text{Re}_6)_{\text{ox}} \cdot 2\text{CD}]^{3-} \quad (5)$$

0.820 V and $K_{11} = 900 \text{ M}^{-1}$, equation 4 leads to $\beta'_2 = 2.2 \cdot 10^7 \text{ M}^2$. This result highlights the high affinity of the oxidized species $[\text{Re}_6\text{S}_8(\text{CN})_6]^{3-}$ for $\gamma\text{-CD}$ while such a global constant β_2 was found negligible for a similar process involving the reduced cluster $[\text{Re}_6\text{S}_8(\text{CN})_6]^{4-}$ (see Table 1). It should be worth noting that for $\gamma\text{-CD}$ equivalent number below 10, analytical treatment remains quite tricky mainly due to i) the presence of different species resulting from the combinations of the redox and host-guest states and ii) the variation of the $\gamma\text{-CD}$ concentration in the diffusion layer as function of applied potential.

Strikingly, the Se- and Te-containing clusters (compounds 2 and 1) behave differently from that previously observed with the sulfur derivative. Thus, gradual addition of $\gamma\text{-CD}$ affects significantly the CVs of the compounds 1 and 2 (shown in Figures 8b-c), by the disappearance of the initial redox waves of the solvated cluster for the benefit of a new anodic potential peak systematically shifted toward lower potential at about 0.480 V and 0.175 V for $\text{Q} = \text{Se}$ and $\text{Q} = \text{Te}$, respectively. Besides, as the $\gamma\text{-CD}$ concentration increases, these new anodic peaks slowly move toward more positive potential values (see Figures 8b-c). Furthermore, while the shape of the oxidation peaks remains almost unchanged in the presence of $\gamma\text{-CD}$, the reverse reduction wave appears totally cancelled for both Se- and Te-containing clusters. Then, as the global redox process appear fully irreversible, the anodic peak currents exhibit a fair linear dependence upon square root of the potential scan rate (see SI §7.1, Figure S12), indicating that the oxidation process remains fast while the reverse reduction becomes extremely slow in the presence of $\gamma\text{-CD}$. Thus, such a redox behavior appears rather consistent with slow formation / dissociation of the host-guest complexes on the time scale experiment. Thus, in the presence of 0.5 equivalent of $\gamma\text{-CD}$, the new anodic peak should correspond to redox process involving the prevalent frozen 1:1 host guest species (see equation 6).



Assuming that Nernst equation pertains, the stability constant of the 1:1 host-guest oxidized species can be estimated from equation 7 where E_a^0 and E_a^{CD} are the anodic peak potential in the absence and in the presence of $\gamma\text{-CD}$, respectively and K'_{11} the stability constant of the oxidized 1:1 host-guest complex.

$$E_a^0 = E_a^{\text{CD}} + 0.059 \log \frac{K'_{11}}{K_{11}} \quad (7)$$

Using experimental values given in Table 1 and 2, K'_{11} values have been determined from equation 7, giving $K'_{11} = 2.4 \cdot 10^5 \text{ M}^{-1}$ and $K'_{11} = 1.0 \cdot 10^7 \text{ M}^{-1}$ for oxidized 1:1 inclusion complexes based on $[\text{Re}_6\text{Se}_8(\text{CN})_6]^{3-}$ and $[\text{Re}_6\text{Te}_8(\text{CN})_6]^{3-}$ clusters, respectively. Then at larger values of $\gamma\text{-CD}$ equivalent number, the anodic peak potential shifts slowly toward positive values to reach limiting values. In this range of composition, speciation curves established from ITC experiments indicate gradual changes of the host-guest composition from 1:1 to 1:2 stoichiometry, thus in such conditions, this limiting anodic peak potential should be close to that of the 1:2 redox couple $[(\text{Re}_6) \cdot 2\text{CD}]^{3-} / [(\text{Re}_6) \cdot \text{2CD}]^{4-}$. Nevertheless, due to the irreversible character of the redox processes supported by the flattening of the anodic peaks observed for large $\gamma\text{-CD}$ equivalents, any straight quantitative analysis remains quite difficult and requires further

FULL PAPER

investigations with regard to the oxidized forms behavior in the presence of the cyclodextrins. However, these preliminary results highlight important electrochemical features that are strongly related to the nature of the inner Q ligands in octahedral cyano clusters $[Re_6Q_8(CN)_6]^{4-3-}$. Importantly, this study reveals that the sulfur-containing cluster leading to the less stable host-guest arrangement behaves as highly dynamic redox host-guest system while features of the other two clusters that exhibit higher host-guest stability are consistent with a frozen redox behavior. Besides, it should be worth mentioning that such a frozen behavior has been previously evidenced by 1H and ^{125}Te NMR for the reduced host-guest complex based on the Te-containing cluster (see Figure 5a). Furthermore, for the three cluster units ($Q = S, Se$ and Te), complexation by γ -CD leads in all cases to the decrease of the half-wave potential, meaning clearly that host-guest affinity of the oxidized species $[Re_6Q_8(CN)_6]^{3-}$ is significantly greater than that of the reduced one $[Re_6Q_8(CN)_6]^{4-}$. Such a trend is nicely supported by quantitative analysis of the electrochemical data summarized in Table 2. Although the full understanding of this observation should require further investigations, especially about the thermodynamic contributors of the solvated oxidized derivatives, reducing of the ionic charge from 4- to 3- should have as main consequence the destabilization of the solvation shell by decreasing ion-dipole interactions. Similar observations were made previously with the ferrocene/ferrocenium as redox active guest interacting with β -CD as host.^[24] Lowering the ionic charge of the guest would make easier the cluster transfer from a solvated to an embedded situation. In other word, the driving force of the encapsulation process should be mainly governed by effective water structure recovery, a process highly orchestrated by the chaotropic nature of the octahedral clusters.

Luminescence properties

The UV-vis spectra of aqueous solutions of $[Re_6S_8(CN)_6]^{4-}$ and $[Re_6Se_8(CN)_6]^{4-}$ are nearly unchanged in the presence of γ -CD. The supramolecular interaction between $[Re_6Te_8(CN)_6]^{4-}$ ion and γ -CD is manifested by only a small red shift of the $[Re_6Te_8(CN)_6]^{4-}$ absorption band from 416 nm to 420 nm (see §8.1 Figure S15).

$[Re_6Q_8(CN)_6]^{4-}$ clusters and their inclusion complexes with γ -CD exhibit luminescence emission spectra in the red/NIR region with almost the same maxima, indicating that the nature of the cluster triplet states is not affected by interaction with γ -CD (see SI §7.2, Figure S16). In all cases, luminescence quantum yields and corresponding lifetimes (i.e., triplet state lifetimes) of inclusion complexes increase when compared with free (unbound) clusters in aqueous solutions. The changes are minor for $[Re_6S_8(CN)_6]^{4-}$, reflecting the weak effects of γ -CD on the cluster as described above (see SI §7.2, Figure S17). In contrast, the formation of inclusion complexes with $[Re_6Se_8(CN)_6]^{4-}$ and $[Re_6Te_8(CN)_6]^{4-}$ clusters enhances luminescence intensities as characterized by increasing luminescence quantum yields and extension of lifetimes (Table 3, see SI §7.2, Figures S16, S17). In the presence of γ -CD, the luminescence decay profile of $[Re_6Se_8(CN)_6]^{4-}$ becomes biphasic with the increasing contribution of a long-lived component at higher γ -CD/ $[Re_6Se_8(CN)_6]^{4-}$ molar ratios (Figure 9B). This behavior may be interpreted by the contribution of at least two species with

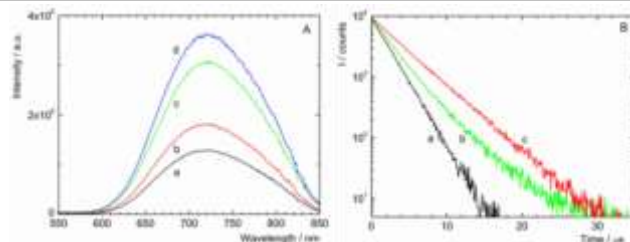


Figure 9. Luminescence properties of $8 \cdot 10^{-5} \text{ mol} \cdot \text{L}^{-1} [Re_6Se_8(CN)_6]^{4-}$ aqueous solutions in the presence of γ -CD in water. A) Luminescence emission spectra in a) air-saturated water, b) oxygen-free water in the absence and in the presence of c) 2.8 or d) 5.4 mM γ -CD. B) Luminescence decay curves a) in oxygen-free water and in the presence of b) 1.0 or c) 5.4 mM γ -CD.

different luminescence lifetimes in the equilibrium, i.e., solvated $[Re_6Se_8(CN)_6]^{4-}$ species and corresponding inclusion complexes with γ -CD. Evidently, the 1:1 and 1:2 complexes are not spectroscopically distinguishable and have the same or very similar luminescence parameters. Nevertheless, introducing a large excess of γ -CD in the cluster solution leads to the recovery of the mono exponential behavior of the emission decay profile, consistent with predominant formation of the 1:2 complex.

The increase of luminescence parameters upon inclusion of the clusters to γ -CD can be attributed to the combination of two factors: exclusion of water molecules from the solvation shell of cluster molecules in the cyclodextrin cavity and reduction of collisional quenching by water molecules from the bulk.^[27] As shown recently by analyzing the magnitude of D_2O/H_2O isotopic effects on the triplet state behavior of these clusters,^[28] energy transfer from their excited states to H_2O vibrational modes leads to extensive non-radiative deactivation. Indeed, due to hydrophobic character inside the cyclodextrin cavity and the fact that water molecules are expelled from the interior and substituted with the cluster body, contacts of excited cluster molecules with water molecules are reduced.

Table 3. Luminescence properties of $[Re_6Q_8(CN)_6]^{4-}$ clusters in water at room temperature: Φ_L is the luminescence quantum yield, $\Phi_{L(CD)}$ is the luminescence quantum yield in the presence of γ -CD ($> 5 \text{ mM}$, measured for excitation wavelengths varying from 340 to 420 nm), τ_0 and τ_{air} are the lifetimes of the triplet states, $\tau_0(CD)$ and $\tau_{air(CD)}$ are the lifetimes of the triplet states of bound clusters with γ -CD ($> 20 \text{ mM}$).

Q	$\Phi_L^{[d]}$	$\Phi_{L(CD)}^{[d]}$	$\tau_0/\mu\text{s}^{[d]}$	$\tau_{air}/\mu\text{s}^{[e]}$	$\tau_0(CD)/\mu\text{s}^{[d]}$	$\tau_{air(CD)}/\mu\text{s}^{[e]}$
S	0.009 ^[a]	< 0.01	1.17 ^[b]	1.06 ^[b]	1.27 ^[b]	1.15 ^[b]
Se	0.015 ^[a]	0.03	2.12 ^[b]	1.50 ^[b]	4.25 ^[b]	2.53 ^[b]
Te	0.004 ^[a]	0.01	0.43 ^[c]	0.34 ^[c]	0.75 ^[c]	0.69 ^[c]

^[a] data from ref. ^[26]. ^[b] Recorded at 720 nm. ^[c] Recorded at 740 nm. ^[d] In oxygen-free water. ^[e] In air-saturated water.

In order to represent accurately how the inclusion of the clusters into the γ -CD cavity affects the efficiency of oxygen quenching of the triplet states, we used the relationship $1 - (\tau_{air}/\tau_0)$ to yield the fraction of the triplet states quenched by oxygen under air-saturated conditions (see Table 3). In agreement with negligible effects of γ -CD on the properties of $[Re_6S_8(CN)_6]^{4-}$, the cluster triplet states of inclusion complex are minimally affected by oxygen with a low fraction of 9%, which is the same as for free

FULL PAPER

$[\text{Re}_6\text{S}_8(\text{CN})_6]^{4-}$. On the other side, the fraction increases from 29 to 40 % in the case of $[\text{Re}_6\text{Se}_8(\text{CN})_6]^{4-}$ inclusion complexes, whereas it decreases from 21 to only 8 % for $[\text{Re}_6\text{Te}_8(\text{CN})_6]^{4-}$ complexes with γ -CD. These effects reflect nicely the fact that while the formation of inclusion complexes increases the lifetimes of the triplet states, thus promoting higher fractions of their quenching by oxygen, it is also accompanied with the drop of diffusion coefficients (see previous paragraph), leading to less effective collisional quenching of the triplet states with oxygen. In the case of $[\text{Re}_6\text{Se}_8(\text{CN})_6]^{4-}$, the increase of the lifetime overcomes the effect of slower diffusion of the inclusion complex. For $[\text{Re}_6\text{Te}_8(\text{CN})_6]^{4-}$ complexes with γ -CD, the increase of the lifetime is limited due to deactivation of the excited states through internal conversion and cannot compensate for slower diffusion, resulting in a small fraction of the triplet states quenched by oxygen.

Conclusions

The self-assembly between native γ -CD and octahedral $[\text{Re}_6\text{Q}_8(\text{CN})_6]^{4-}$ clusters (with Q = S, Se and Te) has been observed and studied both in solid state and in aqueous solution. Varying systematically the inner face-capping chalcogenide ligands of these clusters allowed evidencing key parameters required for the molecular recognition efficiency. In addition to size-fitness, preorganization or attractive host-guest interactions, the chaotropic nature of these clusters should probably have a decisive contribution to the supramolecular association involving water-soluble host and guest species. For instance, the smallest cluster which contains sulfur as inner ligand interacts preferentially with the primary faces of the γ -CD to give a 1:2 supramolecular assembly while the bulkier $[\text{Re}_6\text{Se}_8(\text{CN})_6]^{4-}$ and $[\text{Re}_6\text{Te}_8(\text{CN})_6]^{4-}$ ions appear closely embedded through the secondary faces of the host. Such structural features observed in the solid state from X-ray diffraction analysis are nicely correlated to solution studies which reveals the host-guest stability increases significantly in the following order S < Se < Te. Interestingly, supramolecular interactions provoke significant alterations of the intrinsic physical-chemical properties of the $[\text{Re}_6\text{Q}_8(\text{CN})_6]^{4-}$ clusters such as redox tuning or luminescence enhancement in aqueous solution. Then, the formation of highly stable supramolecular assemblies using functional octahedral clusters (redox and luminescent active) CDs opens a promising way to design advanced multifunctional materials, relevant for photocatalysis or biomedical applications.

Experimental Section

Materials and Methods. All reagents were purchased from commercial sources and used without further purification. $\text{A}_4[\text{Re}_6\text{X}_8(\text{CN})_6]$ ($\text{A} = \text{K}, \text{Na}; \text{X} = \text{S}, \text{Se}, \text{Te}$) were synthesized as described in literature.^[17b, 29]

Fourier Transformed Infrared (FT-IR) spectra were recorded on a Vertex 80 spectrometer. Elemental analyses (C, H, N, S) were carried on an Euro EA 3000 instrument. Energy-dispersive X-ray spectroscopy (EDX) measurements were performed using a SEM-FEG (Scanning Electron Microscope enhanced by a Field Emission Gun) equipment (JSM 7001-F, Jeol). The measures were acquired with a SDD XMax 50 mm² detector and the Aztec (Oxford) system working at 15 kV and 10 mm working

distance. The quantification is realized with the standard library provided by the constructor using La lines. Water and cyclodextrin contents were determined by thermal gravimetric (TGA) analysis with a Mettler Toledo TGA/DSC 1, STAR[®] System apparatus or with a NETZSCH TG 209 F1 device under oxygen flow (50 mL min⁻¹) at a heating rate of 5°C min⁻¹ up to 700°C. NMR studies: All NMR spectra were measured on a Bruker Avance 400 spectrometer in D₂O at 300 K. ¹H and ¹³C NMR spectra were recorded at 400.1 and 100.6 MHz respectively, referenced to the TMS signal. ⁷⁷Se and ¹²⁵Te NMR spectra were measured at Larmor frequencies of 76.3 and 126.3 MHz, using H₂SeO₃ in alkaline solution (1272.6 ppm) and aqueous H₆TeO₆ (713 ppm) as external secondary references, respectively. Translational diffusion measurements were performed using Bruker's "ledbpgs2s" stimulated echo DOSY pulse sequence including bipolar and spoil gradients. Apparent diffusion coefficients were obtained using an adapted algorithm based on the inverse Laplace transform stabilized by maximum entropy.^[30] Electrospray Ionization Mass Spectrometry: Electrospray ionization (ESI) mass spectra were collected using a Q-TOF instrument supplied by WATERS. Samples were solubilized in water at a concentration of 10⁻⁴ M and were introduced into the MS via an ACQUITY UPLC WATERS system whilst a Leucine Enkephalin solution was co-injected via a micro pump as internal standard. Isothermal Titration Calorimetry (ITC): Formation constants and inclusion enthalpies were simultaneously determined for each γ -CD/ $[\text{Re}_6\text{Q}_8(\text{CN})_6]^{4-}$ systems by the use of an isothermal calorimeter (ITC₂₀₀, MicroCal Inc., USA). See supplementary information for further details.

Electrochemistry. Purified water was used throughout. It was obtained by passing water through a RiOs 8 unit followed by a Millipore-Q Academic purification set. All reagents were of high-purity grade and were used as purchased without further purification. Cyclic voltammetric (CV) experiments were carried out with an Methrohm Autolab PGSTAT12 potentiostat/galvanostat associated with a GPES electrochemical analysis system (EcoChemie). Measurements were performed at room temperature in a conventional single compartment cell. A glassy carbon (GC) electrode with a diameter of 3 mm was used as the working electrode. The auxiliary electrode was a Pt plate placed within a fritted-glass isolation chamber and potentials are quoted against a saturated calomel electrode (SCE). The solutions were deaerated thoroughly for at least 30 minutes with pure argon and kept under a positive pressure of this gas during the experiments.

Single-crystal X-ray diffraction analysis. The crystal structures of compound **1** and **2** were determined by X-ray analysis on an Xcalibur (Agilent Technologies) single crystals diffractometer, at 130 K, using graphite-monochromated Mo ($\lambda = 0.71073 \text{ \AA}$) radiation. The reflections intensities were measured ϕ -scanning of narrow (0.5°) frames. Intensity data collection of compound **3** was carried out at $T = 200(2)$ K with a Bruker D8 VENTURE diffractometer equipped with a PHOTON 100 CMOS bidimensional detector using a high brilliance $1\mu\text{s}$ microfocus X-ray Mo Ka monochromatized radiation ($\lambda = 0.71073 \text{ \AA}$). Empirical absorption correction was applied with SCALE3 ABSPACK program^[31] or using the SADABS program.^[32] The structure was solved by direct method and refined with full-matrix least-squares treatment, anisotropically for non-hydrogen atoms in SHEXL^[33] using OLEX2.^[34] Crystals were glued in paratone to prevent any loss of crystallization water. The remaining non-hydrogen atoms were located from Fourier differences and were refined with anisotropic thermal parameters. Positions of the hydrogen atoms belonging to the γ -cyclodextrins were calculated and refined isotropically using the gliding mode. Crystallographic data for **1**: Tetragonal, $I422$, $a=b=23.8046(2)$, $c=57.1588(7)\text{\AA}$, $\alpha=\beta=\gamma=90^\circ$, $V=32389.5(7) \text{ \AA}^3$, $R_1=0.0479$, $wR_2=0.1460$, GOF=1.100 for 15244 independent reflections with $l>2s(l)$. Crystallographic data for **2**: Tetragonal, $I422$, $a=b=23.8608(2)$, $c=57.4481(9) \text{ \AA}$, $\alpha=\beta=\gamma=90^\circ$, $V=32707.4(8) \text{ \AA}^3$, $R_1=0.0534$, $wR_2=0.1622$, GOF= 1.146 for 14796 independent reflections with $l>2s(l)$. Crystallographic data for **3**: Monoclinic, $C2$, $a=63.823(4)$, $b=17.8218(11)$, $c=17.7578(11) \text{ \AA}$, $\alpha=\gamma=90^\circ$ and $\beta=104.248(2)^\circ$, $V=19577(2) \text{ \AA}^3$, $R_1=0.0545$, $wR_2=0.1267$, GOF= 1.034 for 47105 independent reflections

FULL PAPER

with $I > 2s(l)$. For the compounds **1** and **3**, disorder is observed on the encapsulated clusters. In the compound **1**, two positions are observed for $[Re_6Te_8(CN)_6]^{4-}$ (occupancy of site 1 = 94% and occupancy of site 2 = 6%). In this case it was not possible to locate the cyano group of the cluster with occupancy of 6%. In the compound **3**, the encapsulated cluster $[Re_6S_8(CN)_6]^{4-}$ is three fold disordered on three positions (occupancy of site 1 = 90%, occupancy of site 2 = 5%, occupancy of site 3 = 5%). In this, the $[Re_6S_8(CN)_6]^{4-}$ of site 1 is well defined. For the sites 2 and 3, only the $\{Re_6\}$ cores have been located. Selected Crystallographic data for single-crystal X-ray diffraction studies are summarized in Table S1. CCDC-1813565, CCDC-1813564 and CCDC-1813563 for compounds **1**, **2** and **3**, respectively, also contain the supplementary crystallographic data. These data can be obtained free of charge via www.ccdc.cam.ac.uk/data_request/cif.

Optical measurements. UV-vis absorption spectra of solutions were recorded on a Perkin Elmer Lambda 35 spectrometer. Luminescence properties were monitored on a Fluorolog 3 spectrometer equipped with a cooled TBX-05-C photon detection module (Horiba Jobin Yvon). The same instrument was used for luminescence lifetime experiments using an excitation at 390 nm (SpectraLED-390, Horiba Scientific). The decay curves were fitted to exponential functions by the iterative deconvolution procedure of the DAS6 software (v. 6.8, Horiba Jobin Yvon). Absolute photoluminescence quantum yields were measured using a Quantaurus QY C11347-1 spectrometer (Hamamatsu). $8 \cdot 10^{-5}$ mol·L⁻¹ Cluster aqueous solutions were investigated using excitation wavelengths between 340 and 420 nm. For all measurements, oxygen was removed by saturating the solutions with a continuous flow of argon.

Synthesis of $Na_4\{[Re_6Te_8(CN)_6]\subset(\gamma-CD)_2\} \cdot (\gamma-CD) \cdot 30H_2O$ (1). 0.1 g (0.042 mmol) of $Na_4[Re_6Te_8(CN)_6]$ was dissolved in 10 mL of distilled water, after that 0.163 g (0.126 mmol) of γ -CD was added under stirring and gentle heating at 50 °C. Final solution was allowed to slowly evaporate which gave orange cubic crystals of $Na_4\{[Re_6Te_8(CN)_6]\subset(\gamma-CD)_2\} \cdot (\gamma-CD) \cdot 30H_2O$. Yield 0.245 g (86 %) of pure crystalline product. Anal. Calcd for $C_{150}H_{300}Na_4O_{150}Re_6Te_8$: C, 26.42; H, 4.44; N, 1.23. Found: C, 26.5; H, 4.2; N, 1.3. IR (KBr, cm⁻¹): ν = 3406 (s), 2926 (m), 2088 (s), 1639 (s), 1416 (w), 1371 (w), 1337 (w), 1303 (w), 1242 (w), 1157 (m), 1105 (w), 1078 (w), 1024 (s), 999 (w), 941 (w), 850 (w), 760 (w), 707 (w), 581 (w), 528 (w), 405 (w). EDS shows Re : Te : Na ratio = 6 : 7.8 : 3.9. Thermogravimetric analysis revealed a weight loss of about 8% from 50 to 200 °C (the theoretical weight loss of 30 H₂O is 7.93%).

K₄{[Re₆Se₈(CN)₆] \subset (γ -CD)₂} · (γ -CD) · 40H₂O (2). 0.082 g (0.042 mmol) of K₄[Re₆Se₈(CN)₆] was dissolved in 10 mL of distilled water, after that 0.163 g (0.126 mmol) of γ -CD was added under stirring and gentle heating at 50 °C. Final solution was allowed to slowly evaporate which gave orange cubic crystals of K₄{[Re₆Te₈(CN)₆] \subset (γ -CD)₂} · (γ -CD) · 40H₂O. Yield 0.229 g (82 %) of pure crystalline product. Anal. Calcd for $C_{150}H_{290}Na_4K_4O_{145}Re_6Se_8$: C, 28.14; H, 4.56; N, 1.31. Found: C, 28.2; H, 4.4; N, 1.4. IR (KBr, cm⁻¹): ν = 3417 (s), 2926 (m), 2112 (s), 1636 (w), 1413 (w), 1369 (w), 1340 (w), 1305 (w), 1244 (w), 1201 (w), 1159 (m), 1103 (w), 1078 (w), 1024 (s), 997 (w), 941 (w), 856 (w), 760 (w), 708 (w), 580 (w), 530 (w). EDS shows Re : Se : K ratio = 6 : 8.2 : 3.9. Thermogravimetric analysis revealed a weight loss of about 7% from 50 to 200 °C (the theoretical weight loss of 40 H₂O is 7.3%).

Cs₄K₈{[Re₆S₈(CN)₆] \subset (γ -CD)₂} · 2[Re₆S₈(CN)₆] · 2(γ -CD) · 49H₂O (3). 0.1 g (0.059 mmol) of K₄[Re₆S₈(CN)₆] was dissolved in 1 mL of water, after that 0.25 g (0.178 mmol) of γ -CD was dissolved in 1 mL of water and added to cluster solution. After that 0.05 g (0.297 mmol) of CsCl was added to the solution. Then ethanol vapor was allowed to diffuse: a 10 mL vessel containing 2 mL of the final solution of the complex in water was placed into a 250 mL vessel with a tight-fitting lid containing 50 mL of ethanol. The crystals obtained after two days were collected, washed with mixture water/ethanol and dried on air. Yield: 0.15 g (66 %). Anal. Calcd for $C_{210}H_{418}Cs_4K_8N_{18}O_{209}Re_{18}S_{24}$: C, 21.92; H, 3.66; N, 2.19; S, 6.69. Found: C, 22.0; H, 3.8; N, 2.1; S, 6.6. IR (KBr, cm⁻¹): ν = 3417 (s), 2927 (m),

2121 (s), 1639 (w), 1419 (w), 1371 (w), 1338 (w), 1303 (w), 1244 (w), 1159 (m), 1105 (w), 1078 (w), 1024 (s), 999 (w), 941 (w), 854 (w), 760 (w), 707 (w), 608 (w), 583 (w), 526 (w), 409 (w). EDS shows Re : S : K : Cs ratio = 18 : 23.8 : 7.9 : 3.8. Thermogravimetric analysis revealed a weight loss of about 7.7% from 50 to 200 °C (the theoretical weight loss of 49 H₂O is 7.67%).

Acknowledgements

The authors address a special thank to N. B. Kompankov for technical support. The Authors gratefully acknowledge financial support from LIA-CNRS CLUSPOM and LabEx CHARMMMAT. This work was also supported by i) University of Versailles Saint Quentin, ii) CNRS, iii) Région Ile de France through DIM Nano K, iv) the Czech Science Foundation (N° 18-05076S), v) Russian Science Foundation (No. 15-15-10006), vi) Russian Foundation for Basic Research (grant number 17-53-16006), vii) NIIC thanks Federal Agency for Scientific Organizations for funding and viii) A.A. Ivanov thanks Embassy of France in Russia for the Vernadsky scholarship for post-graduate students

Keywords: metal cluster complex • cyclodextrin • supramolecular self-assembly • luminescence • electrochemistry

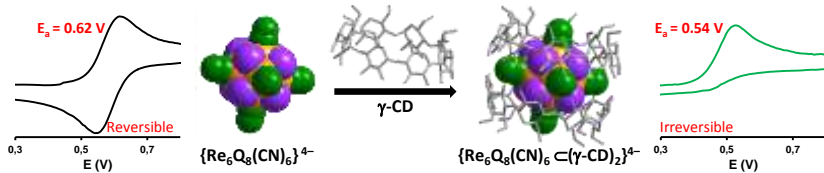
- [1] D. B. Walker, G. Joshi, A. P. Davis, *Cell. Mol. Life Sci.* **2009**, *66*, 3177-3179.
- [2] a) M. M. Boyle, R. A. Smaldone, A. C. Whalley, M. W. Ambrogio, Y. Y. Botros, J. F. Stoddart, *Chem. Sci.* **2011**, *2*, 204-210; b) A. de la Escosura-Muñiz, A. Merkoçi, *ACS Nano* **2012**, *6*, 7556-7583.
- [3] A. Magnuson, M. Anderlund, O. Johansson, P. Lindblad, R. Lomoth, T. Polivka, S. Ott, K. Stensjö, S. Styring, V. Sundström, L. Hammarström, *Acc. Chem. Res.* **2009**, *42*, 1899-1909.
- [4] A. J. Neel, M. J. Hilton, M. S. Sigman, F. D. Toste, *Nature* **2017**, *543*, 637-646.
- [5] a) A. Müller, P. Gouzerh, *Chem. Soc. Rev.* **2012**, *41*, 7431-7463; b) R. A. Smaldone, R. S. Forgan, H. Furukawa, J. J. Gassensmith, A. M. Z. Slawin, O. M. Yaghi, J. F. Stoddart, *Angew. Chem.-Int. Ed.* **2010**, *49*, 8630-8634.
- [6] a) T. R. Cook, Y.-R. Zheng, P. J. Stang, *Chem. Rev.* **2013**, *113*, 734-777; b) J. Marrot, M. A. Pilette, M. Haouas, S. Floquet, F. Taulelle, X. López, J. M. Poblet, E. Cadot, *J. Am. Chem. Soc.* **2012**, *134*, 1724-1737; c) Y. Molard, *Acc. Chem. Res.* **2016**, *49*, 1514-1523.
- [7] F. Hapiot, H. Bricout, S. Menuel, T. S., E. Monflier, *Catal. Sci. Technol.* **2014**, *4*, 1899-1908.
- [8] a) K. Benner, P. Klüfers, J. Schuhmacher, *Angew. Chem.-Int. Ed.* **1997**, *36*, 743-745; b) M. O'Keeffe, O. M. Yaghi, *Chem. Rev.* **2012**, *112*, 675-702.
- [9] a) M. Chen, L. Cui, C. Li, G. Diao, *J. Hazard. Mater.* **2009**, *162*, 23-28; b) A. Harada, Y. Takashima, M. Nakahata, *Acc. Chem. Res.* **2014**, *47*, 2128-2140; c) E. Karakhanov, A. L. Maksimov, A. V. Zolotukhina, Y. S. Kardasheva, *Russ. Chem. Bull.* **2013**, *62*, 1465-1492; d) Z. Liu, A. Samanta, J. Lei, J. Sun, Y. Wang, J. F. Stoddart, *J. Am. Chem. Soc.* **2016**, *138*, 11643-11653.
- [10] R. Gramage-Doria, D. Arnsbach, D. Matt, *Coord. Chem. Rev.* **2013**, *257*, 776-816.
- [11] L. Leclercq, A. R. Schmitzer, *Organometallics* **2010**, *29*, 3442-3449.
- [12] a) M. A. Moussawi, M. Haouas, S. Floquet, W. E. Shepard, P. A. Abramov, M. N. Sokolov, V. P. Fedin, S. Cordier, A. Ponchel, E. Monflier, J. Marrot, E. Cadot, *J. Am. Chem. Soc.* **2017**, *139*, 14376-14379; b) M. A. Moussawi, N. Leclerc-Laronze, S. Floquet, P. A. Abramov, M. N. Sokolov, S. Cordier, E. Monflier, H. Bricout, D. Landy, M. Haouas, J. Marrot, E. Cadot, *J. Am. Chem. Soc.* **2017**, *139*, 12793-12803; c) Y. Wu, R. Shi, Y.-L. Wu, J. M. Holcroft, Z. Liu, M. Frasconi, M. R. Wasielewski, H. Li, J. F. Stoddart, *J. Am. Chem. Soc.* **2015**, *137*, 4111-4118; d) L. Yue, S. Wang, D. Zhou, H. Zhang, B. Li, L. Wu, *Nat.*

FULL PAPER

- Commun.* **2016**, *7*, 10742-10752; e) B. Zhang, W. Guan, F. Yin, J. Wang, B. Li, L. Wu, *Dalton Trans.* **2018**, *47*, 1388-1392; f) B. Zhang, L. Yue, Y. Wang, Y. Yang, L. Wu, *Chem. Commun.* **2014**, *50*, 10823-10826.
- [13] a) P. A. Abramov, A. A. Ivanov, M. A. Shestopalov, M. A. Moussawi, E. Cadot, S. Floquet, M. Haouas, M. N. Sokolov, *J. Clust. Sci.* **2018**, *29*, 9-13; b) K. Kirakci, V. Šícha, J. Holub, P. Kubát, K. Lang, *Inorg. Chem.* **2014**, *53*, 13012-13018.
- [14] a) M. Amela-Cortes, A. Garreau, S. Cordier, E. Faulques, J.-L. Duvail, Y. Molard, *J. Mater. Chem. C* **2014**, *2*, 1545-1552; b) M. Amela-Cortes, Y. Molard, S. Paofai, A. Desert, J. L. Duvail, N. G. Naumov, S. Cordier, *Dalton Trans.* **2016**, *45*, 237-245; c) O. A. Efremova, Y. A. Vorotnikov, K. A. Brylev, N. A. Vorotnikova, I. N. Novozhilov, N. V. Kuratieva, M. V. Edeleva, D. M. Benoit, N. Kitamura, Y. V. Mironov, M. A. Shestopalov, A. J. Sutherland, *Dalton Trans.* **2016**, *45*, 15427-15435; d) R. El Osta, A. Demont, N. Audebrand, Y. Molard, T. T. Nguyen, R. Gautier, K. A. Brylev, Y. V. Mironov, N. G. Naumov, N. Kitamura, S. Cordier, *Z. Anorg. Allg. Chem.* **2015**, *641*, 1156-1163; e) K. Kirakci, P. Kubát, K. Fejfarová, J. Martinčík, M. Nikl, K. Lang, *Inorg. Chem.* **2016**, *55*, 803-809; f) M. A. Mikhailov, K. A. Brylev, P. A. Abramov, E. Sakuda, S. Akagi, A. Ito, N. Kitamura, M. N. Sokolov, *Inorg. Chem.* **2016**, *55*, 8437-8445; g) L. Riehl, A. Seyboldt, M. Ströbele, D. Enseling, T. Jüstel, M. Westberg, P. R. Ogilby, H.-J. Meyer, *Dalton Trans.* **2016**, *45*, 15500-15506; h) M. N. Sokolov, K. A. Brylev, P. A. Abramov, M. R. Gallyamov, I. N. Novozhilov, N. Kitamura, M. A. Mikhailov, *Eur. J. Inorg. Chem.* **2017**, *4131*-4137.
- [15] a) A. M. Cheplakova, A. O. Solovieva, T. N. Pozmogova, Y. A. Vorotnikov, K. A. Brylev, N. A. Vorotnikova, E. V. Vorontsova, Y. V. Mironov, A. F. Poveshchenko, K. A. Kovalenko, M. A. Shestopalov, *J. Inorg. Biochem.* **2017**, *166*, 100-107; b) E. V. Svezhentseva, A. O. Solovieva, Y. A. Vorotnikov, O. G. Kurskaya, K. A. Brylev, A. R. Tsygankova, M. V. Edeleva, S. N. Gyrylova, N. Kitamura, O. A. Efremova, M. A. Shestopalov, Y. V. Mironov, A. M. Shestopalov, *New J. Chem.* **2017**, *41*, 1670-1676.
- [16] a) S.-J. Choi, K. A. Brylev, J.-Z. Xu, Y. V. Mironov, V. E. Fedorov, Y. S. Sohn, S.-J. Kim, J.-H. Choy, *J. Inorg. Biochem.* **2008**, *102*, 1991-1996; b) A. A. Krasilnikova, A. O. Solovieva, K. E. Trifonova, K. A. Brylev, A. A. Ivanov, S.-J. Kim, M. A. Shestopalov, M. S. Fufaeva, A. M. Shestopalov, Y. V. Mironov, A. F. Poveshchenko, L. V. Shestopalova, *Contrast Media Mol. Imaging* **2016**, *11*, 459-466.
- [17] a) A. A. Krasilnikova, M. A. Shestopalov, K. A. Brylev, I. A. Kirilova, O. P. Khripko, K. E. Zubareva, Y. I. Khripko, V. T. Podorognaya, L. V. Shestopalova, V. E. Federov, Y. V. Mironov, *J. Inorg. Biochem.* **2015**, *144*, 13-17; b) A. A. Krasilnikova, A. O. Solovieva, A. A. Ivanov, K. E. Trifonova, T. N. Pozmogova, A. R. Tsygankova, A. I. Smolentsev, E. I. Kretov, D. S. Sergeevichev, M. A. Shestopalov, Y. V. Mironov, A. M. Shestopalov, A. F. Poveshchenko, L. V. Shestopalova, *Nanomedicine: NBM* **2017**, *13*, 755-763.
- [18] a) A. Beltrán, M. Mikhailov, M. N. Sokolov, V. Pérez-Laguna, A. Rezusta, M. José Revillo, F. Galindo, *J. Mater. Chem. B* **2016**, *4*, 5975-5979; b) C. Felip-León, C. Arnau del Valle, V. Pérez-Laguna, M. I. Millán-Lou, J. F. Miravet, M. Mikhailov, M. N. Sokolov, A. Rezusta-López, F. Galindo, *J. Mater. Chem. B* **2017**, *5*, 6058-6064; c) A. O. Solovieva, Y. A. Vorotnikov, K. E. Trifonova, O. A. Efremova, A. A. Krasilnikova, K. A. Brylev, E. V. Vorontsova, P. A. Avrorov, L. V. Shestopalova, A. F. Poveshchenko, Y. V. Mironov, M. A. Shestopalov, *J. Mater. Chem. B* **2016**, *4*, 4839-4846.
- [19] J. Szewczyk, *Med. Res. Rev.* **1994**, *14*, 353-386.
- [20] K. I. Assaf, M. S. Ural, F. Pan, T. Georgiev, S. Simova, K. Rissanen, D. Gabel, W. M. Nau, *Angew. Chem.-Int. Ed.* **2015**, *54*, 6852-6856.
- [21] a) Y. V. Mironov, J. A. Cody, T. E. Albrecht-Schmitt, J. A. Ibers, *J. Am. Chem. Soc.* **1997**, *119*, 493-498; b) H.-J. Schneider, F. Hacket, V. Rüdiger, H. Ikeda, *Chem. Rev.* **1998**, *98*, 1755-1785.
- [22] A. J. M. Valente, R. A. Carvalho, O. Söderman, *Langmuir* **2015**, *31*, 6314-6320.
- [23] M. V. Rekharsky, Y. Inoue, *Chem. Rev.* **1998**, *98*, 1875-1917.
- [24] T. Matsue, D. H. Evans, T. Osa, N. Kobayashi, *J. Am. Chem. Soc.* **1985**, *107*, 3411-3417.
- [25] W. A. Rabanal-León, J. A. Murillo-López, D. Páez-Hernández, R. Arratia-Pérez, *J. Phys. Chem. A* **2014**, *118*, 11083-11089.
- [26] T. Yoshimura, S. Ishizaka, Y. Sasaki, H.-B. Kim, N. Kitamura, N. G. Naumov, M. N. Sokolov, V. E. Federov, *Chem. Lett.* **1999**, *28*, 1121-1122.
- [27] K. Lang, J. Mosinger, D. M. Wagnerová, *Coord. Chem. Rev.* **2004**, *248*, 321-350.
- [28] A. O. Solovieva, K. Kirakci, A. A. Ivanov, P. Kubát, T. N. Pozmogova, S. M. Miroshnichenko, E. V. Vorontsova, A. V. Chechushkov, K. E. Trifonova, M. S. Fufaeva, E. I. Kretov, Y. V. Mironov, A. F. Poveshchenko, K. Lang, M. A. Shestopalov, *Inorg. Chem.* **2017**, *56*, 13491-13499.
- [29] a) H. Imoto, N. G. Naumov, A. V. Virovets, T. Saito, V. E. Federov, *J. Struct. Chem.* **1998**, *39*, 720-727; b) N. G. Naumov, S. B. Artemkina, A. V. Virovets, V. E. Fedorov, *Solid State Sci.* **1999**, *1*, 473-481; c) N. G. Naumov, A. V. Virovets, N. V. Podberezhskaya, V. E. Federov, *J. Struct. Chem.* **1997**, *38*, 857-862.
- [30] M. A. Delsuc, T. E. Mallia, *Anal. Chem.* **1998**, *70*, 2146-2148.
- [31] Oxford Diffraction. *CrysAlis CCD and CrysAlis RED, including ABSPACK Versions 1.171.32.3 2006*.
- [32] G. M. Sheldrick, *SADABS, program for scaling and correction of area detector data, University of Göttingen, Germany* **1997**.
- [33] G. M. Sheldrick, *Acta Cryst. C* **2015**, *71*, 3-8.
- [34] O. V. Dolomanov, L. J. Bourhis, R. J. Gildea, J. A. K. Howard, H. Puschmann, *J. Appl. Cryst.* **2009**, *42*, 339-341.

FULL PAPER

FULL PAPER



Supramolecular recognition dictated by chaotropic effect. Water-soluble $[\text{Re}_6\text{Q}_8(\text{CN})_6]^{4-}$ ($\text{Q} = \text{S}, \text{Se}, \text{Te}$) octahedral clusters react with γ -cyclodextrin producing supramolecular inclusion systems. The nature of the inner Q ligands influences strongly the water structure - breaking character of the clusters, resulting in different host-guest stability. The encapsulation modifies significantly the intrinsic physical-chemical properties of the inorganic guest (redox & luminescence).

A.A. Ivanov, C. Falaise, P.A. Abramov,*
M.A. Shestopalov, K. Kirakci, K. Lang,
M.A. Moussawi, M.N. Sokolov, N.G.
Naumov, S. Floquet, D. Landy, M.
Haouas,* K.A. Brylev, Y.V. Mironov, Y.
Molard, S. Cordier and E. Cadot*

Page No. – Page No.

Host-Guest Binding Hierarchy within Redox- and Luminescence Responsive Supramolecular Self-Assembly Based on Chalcogenide Clusters and γ -Cyclodextrin